

See discussions, stats, and author profiles for this publication at: <https://www.researchgate.net/publication/6549890>

A Two-Step Spin Transition with a Disordered Intermediate State in a New Two-Dimensional Coordination Polymer

ARTICLE *in* THE JOURNAL OF PHYSICAL CHEMISTRY B · MARCH 2007

Impact Factor: 3.3 · DOI: 10.1021/jp066010p · Source: PubMed

CITATIONS

45

READS

57

6 AUTHORS, INCLUDING:



J.A. Rodriguez-Velamazán

Materials Science Institute of Aragon, Zaragoza...

68 PUBLICATIONS 498 CITATIONS

SEE PROFILE



Miguel Castro

University of Zaragoza

69 PUBLICATIONS 1,242 CITATIONS

SEE PROFILE



Ramon Burriel

Spanish National Research Council

166 PUBLICATIONS 1,784 CITATIONS

SEE PROFILE



Takafumi Kitazawa

Toho University

102 PUBLICATIONS 1,246 CITATIONS

SEE PROFILE

ARTICLES

A Two-Step Spin Transition with a Disordered Intermediate State in a New Two-Dimensional Coordination Polymer

J. Alberto Rodríguez-Velamazán, Miguel Castro,* Elías Palacios, and Ramón Burriel

Instituto de Ciencia de Materiales de Aragón, CSIC - Universidad de Zaragoza, Pedro Cerbuna 12, 50009 Zaragoza, Spain

Takafumi Kitazawa and Takeshi Kawasaki

*Department of Chemistry, Faculty of Science, Toho University, Miyama, Funabashi, Chiba, 274-8510, Japan**Received: September 14, 2006; In Final Form: November 30, 2006*

The two-dimensional (2D) polymeric spin crossover (SCO) compound $\text{Fe}(\text{py})_2[\text{Ag}(\text{CN})_2]_2$ has been synthesized. The compound shows a two-step spin transition detected by magnetic, heat capacity, and X-ray diffraction measurements. The magnetic moment shows a high-temperature step (step 1) occurring at 146.3 K without hysteresis, while the low-temperature step (step 2) happens at 84 K on cooling and 98.2 K on heating. These measurements reveal a large amount of residual high spin (HS) species (23%) and that HS state trapping occurs at cooling rates of around 1 K min^{-1} or higher. The two-step behavior has been confirmed by heat capacity, which gives, for steps 1 and 2, respectively, $\Delta H_1 = 3.33 \text{ kJ mol}^{-1}$, $\Delta S_1 = 22.6 \text{ J mol}^{-1} \text{ K}^{-1}$, and $\Delta H_2 = 1.51 \text{ kJ mol}^{-1}$, $\Delta S_2 = 15.7 \text{ J mol}^{-1} \text{ K}^{-1}$. For step 2 a hysteresis of 10 K has been determined with dynamic measurements. Powder X-ray diffraction at room temperature shows that the compound is isostructural to $\text{Cd}(\text{py})_2[\text{Ag}(\text{CN})_2]_2$ previously reported. Powder X-ray diffraction indicates that there is only one crystallographic site for iron(II) in the whole temperature range, confirmed by Mössbauer spectroscopy. The X-ray diffraction study at different temperatures do not show any superstructure in the region between the transitions, discarding a crystallographic phase transition as the origin of the two-step behavior. However, an unexpected increase of the thermal factor is detected on lowering the temperature and considered as a manifestation of a disordered state between the two steps, consisting of a mixing of HS and LS species without long-range order.

I. Introduction

In spin crossover (SCO) compounds, transition metal ions (being iron(II) the most common one) undergo a spin conversion, when the temperature changes, between high spin (HS) and low spin (LS) states. The intensity of the cooperativity between the SCO sites gives rise to different magnetic spin crossover behaviors,¹ described by the HS fraction, which can be continuous or discontinuous and even show hysteresis when the cooperativity is strong enough. The existence of hysteresis and, therefore, bistability, opens application possibilities in areas like sensors, molecular switches, and data storage devices.²

The spin conversion may also occur as a two-step curve,¹ and therefore, with an intermediate state between the HS state at high temperatures and the LS state at low temperatures. This behavior has been a challenge for a theoretical explanation and has attracted considerable attention in spite of the few examples reported in the literature.

The origin of the two-step transition in both mononuclear and polymeric compounds³ is mostly due to the presence of two or more lattice sites with different SCO transition temper-

atures.⁴ This multiple site for the SCO ion can exist at room temperature or be produced by some lower temperature structural transition. Dinuclear compounds can also show the two-step transition. Structural analysis from Amore et al.⁵ showed ordered HS–LS molecules at the intermediate plateau coming from the different geometries around the two iron atoms in the molecular unit. In other cases,^{6,7} the combined effect of elastic intramolecular interactions (antiferromagnetic-like) and cooperative intermolecular interactions (ferromagnetic-like) is responsible for the magnetic behavior.

The most studied two-step SCO compound has been $[\text{Fe}(\text{2-pic})_3]\text{Cl}_2\text{EtOH}$ (2-pic = 2-picolyamine).⁸ This compound was initially considered as the example of a two-step transition with an intermediate state built from ordered clusters of HS–LS pairs, with a correlation length comparable to the next-nearest neighbor distances and, therefore, without long-range ordering.⁹ The fact that a unique iron crystallographic site was determined in both the HS and LS states suggested that this behavior could be due to a competition between long-range ferromagnetic-type and short-range antiferromagnetic-type interactions. A new sight appeared when Chernyshov et al.¹⁰ reinvestigated this compound with X-ray diffraction and detected a superstructure inside the temperature range of the intermediate state, indicating the

* To whom all correspondence should be addressed. Phone: 34-976762528; fax: 34-976761957, e-mail: mcastro@unizar.es.

presence of two nonequivalent iron(II) sites and a long-range order of the HS and LS molecules. However, Kusz et al.¹¹ have not detected the expected superstructure during the decay of the metastable HS state induced after irradiation with green light (514 nm) at 10 K. In 2004, Grunert et al.¹² reported a new polymeric SCO compound with a three-dimensional structure. Their compound undergoes a two-step transition with only one crystallographic site for iron(II) in the whole temperature range, confirmed by X-ray diffraction and Mössbauer spectroscopy. The coexistence of HS and LS species between the two steps is supported by a considerable elongation of the displacement ellipsoids of the N atoms around iron(II). Some examples of two-step spin transition have been reported where order–disorder phenomena seems to play an important role in the SCO behavior.¹³ Recently, Matouzenko et al.¹⁴ have reported a mononuclear complex with a unique iron(II) crystallographic site which undergoes a two-step transition without structural transition. The two-step behavior is here related with the two different geometries of the FeN₆ coordination core generated by an order–disorder phenomenon in the ligand.

Our compound, Fe(py)₂[Ag(CN)₂]₂, follows the same synthetic strategy of other Hofmann-like clathrate compounds previously reported, like Fe(py)₂[Ni(CN)₄]₁₅ and Fe(3-CNpy)₂[Ag(CN)₂]₂,¹⁶ in the search of more versatile systems with a improved communication between the active SCO centers. In this paper we report the study of this polymeric compound by powder X-ray diffraction, magnetic, Mössbauer spectroscopy, and calorimetric measurements. This is the first compound with two-dimensional topology showing a two-step spin transition.

II. Experimental Section

Fe(py)₂[Ag(CN)₂]₂ was prepared by the method applied for Cd(py)₂[Ag(CN)₂]₂.¹⁷ Under N₂ gas, L(+)-ascorbic acid (0.44 g) and pyridine (1 mL) were dissolved into water (35 mL). We added 0.49 g of Mohr salt Fe(NH₄)₂(SO₄)₂·6H₂O and K[Ag(CN)₂] (0.50 g) to this solution. Yellow powder crystals precipitated immediately. The precipitate was filtered through a membrane. Elemental analysis gives (found/calc %): C, 31.42/31.50; H, 1.88/1.88; N 15.57/15.75.

Powdered samples of around 13 mg were measured on a MPMS-XL Quantum Design SQUID magnetometer between 5 and 300 K on both cooling and heating modes, at different rates, in an external field of 1 T.

⁵⁷Fe Mössbauer experiments were carried out on powder samples on cooling from 290 to 90 K on a Wissel Mössbauer spectrometer consisting on a MDU-1200 driving unit and a MVT-100 velocity transducer, incorporating a Seiko model 7800 multichannel analyzer. The sample (60 mg) was kept in a Heli-Tan LT-3 gas-flow cryostat (Advanced Research System Inc.) equipped with a 9620 digital temperature controller from Scientific Instruments, and the ⁵⁷Co(Rh) source was maintained at room temperature.

Heat capacity measurements have been performed in a commercial adiabatic calorimeter from Termis Ltd.¹⁸ A powdered sample of 48.12 mg was sealed in an oxygen-free copper vessel whose contribution (known by a separate experiment) was subtracted from the total heat capacity in order to obtain C_p of the sample. The conventional heat pulse method was used to obtain C_p values. To map the transition on heating and cooling and to estimate the thermal hysteresis, a dynamic procedure was used.¹⁹

X-ray diffraction patterns were taken at different temperatures between RT and 80 K, using a Cu rotating anode generator operated at 35 kV, 80 mA. The Kα₁ + Kα₂ pair was selected

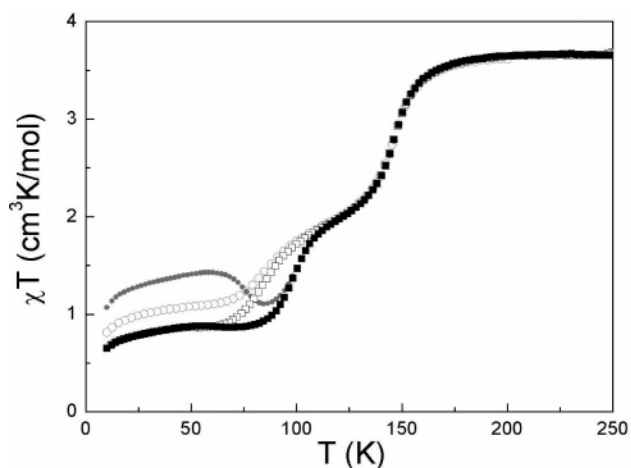


Figure 1. Magnetic behavior of Fe(py)₂[Ag(CN)₂]₂ shown as χT vs T . Cooling at 0.35 K min⁻¹ (□) and subsequent heating at 1 K min⁻¹ (■). Cooling at 1 K min⁻¹ (○) and heating at 1 K min⁻¹ (●) after a rapid cooling (10 K min⁻¹).

by a graphite monochromator. A D-max Rigaku diffractometer was used as detector, in steps of 0.03°. Data have been analyzed using the FULLPROF program.²⁰

III. Results and Discussion

III.A. Magnetic Measurements. The magnetic behavior of Fe(py)₂[Ag(CN)₂]₂ is shown in Figure 1, using the χT product versus temperature representation (where χ stands for the magnetic susceptibility), for cooling and heating measurements performed at various rates. These curves reveal a spin conversion occurring in two steps. At high temperature, this product reaches 3.66 cm³ K mol⁻¹ in agreement with the expected values for a HS iron(II) ion. As the temperature decreases, a constant value is maintained down to around 180 K followed by a large decrease to 2.25 cm³ K mol⁻¹ at 135 K (step 1). Between 135 and 110 K, χT shows a smooth decrease defining a small plateau, and finally, below 110 K, it falls reaching a value which depends on the cooling rate (step 2). This value is 0.85, 1.08, and 1.4 cm³ K mol⁻¹ at 50 K for cooling rates of 0.35, 1, and 10 K min⁻¹, respectively. Therefore, after the spin transition there is a presence of HS species, and thermal trapping of the HS state exists if the cooling rate is high enough. The decrease of the magnetic moment at lower temperatures is most likely due to the zero-field splitting of the HS species, as often happens in SCO compounds.

A heating measurement performed at 1 K min⁻¹ after the fast cooling shows the HS–LS relaxation at 75 K, while this process cannot be seen on the heating curve after the slowest cooling rate. Therefore, there is a residual HS fraction of around 23% and an additional 7% and 16% of HS species are trapped with cooling rates of 1 and 10 K min⁻¹, respectively. This trapping is usually associated²¹ with the presence of a crystallographic phase transition but it can also exist if the HS to LS relaxation at the thermal spin transition temperature is slow enough, which is the case in [Fe(mtz)₆](BF₄)₂.²² Therefore, considering that the structural transition is discarded by our X-ray experiments (see the following), the local distribution of the plateau is probably frozen by the rapid cooling.

In the heating measurement performed at 1 K min⁻¹ after the slowest cooling, step 2 appears at higher temperature, showing a thermal hysteresis which indicates a first-order character for this step of the transition, while the high-temperature step remains identical. The transition temperatures are $T_1 = 146.3$ K for step 1, $T_{2,up} = 98.2$ K and $T_{2,down} = 84$ K

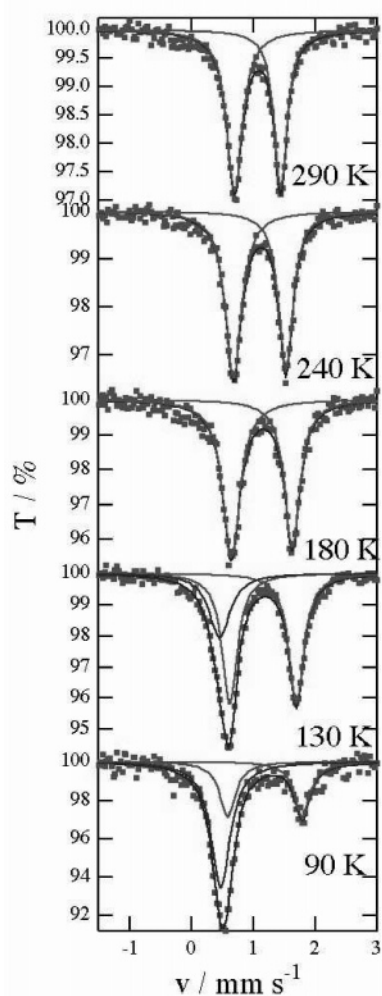


Figure 2. Mössbauer spectra of $\text{Fe}(\text{py})_2[\text{Ag}(\text{CN})_2]_2$ at selected temperatures.

TABLE 1: Mössbauer Parameters for $\text{Fe}(\text{py})_2[\text{Ag}(\text{CN})_2]_2$

<i>T</i> (K)	site	I.S. (mm s ⁻¹)	Q.S. (mm s ⁻¹)	Γ_{exp} (mm s ⁻¹)	HS fraction (%)
290	HS	1.07	0.74	0.31	100
240	HS	1.11	0.85	0.30	100
180	HS	1.14	0.98	0.34	100
130	HS	1.16	1.07	0.30	74(3)
	LS	0.46		0.42	26(3)
90	HS	1.19	1.20	0.31	42(3)
	LS	0.48		0.38	58(3)

for the heating (at 1 K min⁻¹) and cooling (at 0.35 K min⁻¹) processes for step 2, respectively. The spin conversions of the high and low-temperature steps correspond to 45% and 32% of the iron(II) sites, respectively.

III.B. Mössbauer Spectroscopy. The Mössbauer spectra of a powder sample of $\text{Fe}(\text{py})_2[\text{Ag}(\text{CN})_2]_2$ were recorded at temperatures between 90 and 290 K (Figure 2) and the results are in agreement with the magnetic data. The obtained Mössbauer parameters and the deduced HS fraction are listed in Table 1. The spectra were analyzed with a doublet for the HS site and a singlet for the LS site. At low temperature, where HS and LS species coexist, the fit has been done considering the same width, Γ_{exp} , for both lines of the HS doublet, while at high temperature, a different Γ_{exp} is considered for each line.

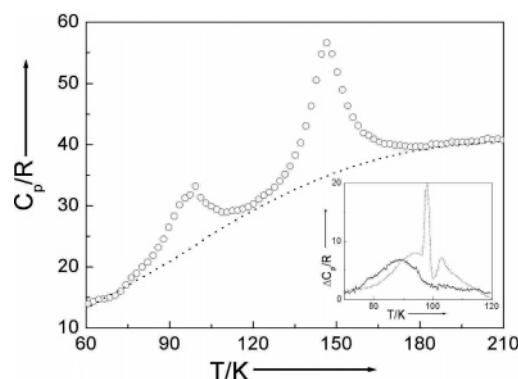


Figure 3. Heat capacity of $\text{Fe}(\text{py})_2[\text{Ag}(\text{CN})_2]_2$ in the spin transition temperature range obtained by adiabatic calorimetry. The dotted line stands for the estimated non-anomalous heat capacity. Inset: Anomalous heat capacity obtained with dynamic measurements of step 2 on heating (dotted line) and on cooling (continuous line).

Isomer shifts (IS) were given relative to α -Fe at room temperature. The data of the HS fraction were obtained assuming equal Mössbauer–Lamb factors for HS and LS states. The isomer shift and quadrupole splitting (QS) values at 290, 240, and 180 K indicate that the iron(II) ions are in one kind of HS sites and the Mössbauer spectra at 130 and 90 K show that one kind of HS states and one kind of LS states coexist. No evidence of iron(III) impurities is found in these results.

III.C. Heat Capacity. The heat capacity values obtained by adiabatic calorimetry are shown in Figure 3. The curve shows two peaks at 146.5 and 99 K in accordance with magnetic measurements. After subtracting a smooth non-anomalous contribution, the enthalpy and entropy variations associated to step 1 are $\Delta H_1 = 3.33 \text{ kJ mol}^{-1}$, $\Delta S_1 = 22.6 \text{ J mol}^{-1}\text{K}^{-1}$ and the magnitudes associated to step 2, $\Delta H_2 = 1.51 \text{ kJ mol}^{-1}$, $\Delta S_2 = 15.7 \text{ J mol}^{-1}\text{K}^{-1}$. Considering that the total values of enthalpy and entropy stand for about 77% of spin conversion, the complete transition would give $\Delta H = 6.29 \text{ kJ mol}^{-1}$, $\Delta S_2 = 49.7 \text{ J mol}^{-1}\text{K}^{-1}$, that lie in the lower range of the generally observed values.²³ The fraction of the observed entropy of step 2 represents 31% of the overall entropy, in agreement with magnetic results. Dynamic measurements¹⁹ have been done in the same temperature range at a scan rate of less than 0.15 K min⁻¹ on cooling and heating. The inset of Figure 3 only shows the data of step 2 since, in agreement with the magnetic behavior, no hysteresis has been detected for step 1. The thermal hysteresis of around 10 K, similar to the one observed by magnetic measurements, indicates a first-order character. The difference between the measured temperature of the calorimetric vessel and the real temperature of the sample has been estimated to be of less than 1 K, which discards a kinetic origin for the hysteresis.

III.D. X-ray Diffraction. Our compound results to be isostructural with a derived one in which Cd replaces Fe, whose crystal structure has been solved by single-crystal X-ray diffraction.¹⁷ Therefore, the starting parameters for the X-ray powder diffraction analysis have been taken from the structure of the Cd compound. The structure has been refined by imposing soft constraints to the C–C, C–N, and C–H distances (limited within a standard deviation of 0.02 Å), preserving the shape of the pyridine molecule and the cyanide bond length, in order to reduce the number of refinable parameters. Values are taken from current literature.²⁴ The refinement allowed us to determine the Fe–N distances quite well from powder patterns. An overall “thermal” parameter has also been used. At temperatures above 200 K the refinement converges and gives a good calculation—

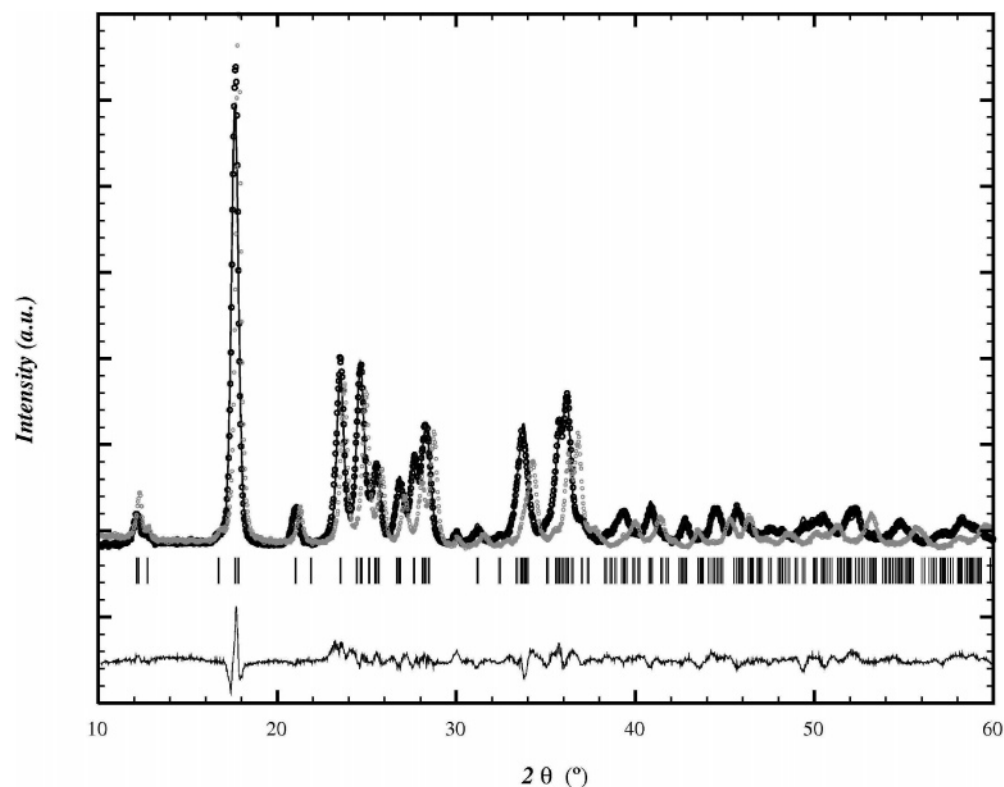


Figure 4. X-ray diffraction patterns at 200 K (black symbols) and 100 K (gray symbols), and Rietveld refinement at 200 K (continuous line), using the structural model of $\text{Cd}(\text{py})_2[\text{Ag}(\text{CN})_2]_2$ as starting parameters and imposing soft constraints to C–C and C–N distances. Ticks are the positions of the Bragg reflections.

experimental agreement (see Figure 4 for the diffraction pattern at 200 K) with the exception of a peak at $2\theta = 30.0^\circ$ which has been identified as the most intense reflection (110) of $\text{Ag}(\text{CN})$, a small byproduct of the synthesis. The average Fe–N distance, $\langle d(\text{Fe} - \text{N}) \rangle = 2.24(2) \text{ \AA}$, is slightly higher than usual for the HS state.¹ An unusually large thermal parameter is observed, probably due to the too restrictive constraints (but the refinement diverges if all the atomic coordinates are left free) or may be due to some disorder in the atomic positions.

As shown in Figure 5, the iron(II) ion is coordinated to four N atoms of the CN group and two N atoms of the pyridine ligand. The polymeric structure of $\text{Fe}(\text{py})_2[\text{Ag}(\text{CN})_2]_2$ involves a two-dimensional $\text{Fe}(\text{NCAgCN}-\text{Fe}_{1/4})_4$ network with a rhombus mesh from which a pair of unidentate pyridine ligands protrude at the trans positions of the iron(II) ion. It has a simple layer structure of stacked 2D networks, whose mesh is penetrated by the py ligands from the upper and lower layers. There is only one crystallographic site for iron(II) in the structure at room temperature.

On lowering the temperature, the structural parameters change, but no modification of the structure type is observed (see Table 2). In the 200 K structure there are two equivalent iron(II) ions in the unit cell related by the base centering of the $C2/m$ space group. Magnetic measurements suggest that the plateau contains around one-half of the iron ions in HS state and another half in LS state. If these HS and LS ions were distributed in a spatially ordered way, a structural transition would be expected between 125 and 180 K making both iron ions nonequivalent by losing the C centering or doubling the unit cell. The loss of the C centering would produce new reflections with $h + k = 2n + 1$ and the doubling of the cell some reflections with half-odd indexes, but our experimental diffraction patterns do not reveal these superstructures. The

average Fe–N distances at 125 K, $\langle d(\text{Fe} - \text{N}) \rangle = 2.17(2) \text{ \AA}$, are lower than at 200 K, but still quite above the expected value for a LS state (2.0 \AA),¹ consistent with a random mixing of iron(II) ions in LS and HS states. The volume change of the unit cell on cooling at a rate of around 0.8 K min^{-1} is depicted in Figure 6, showing the two step behavior. This volume change between 77 and 200 K is $\Delta V = 63.9(6) \text{ \AA}^3$, or $32.0(3) \text{ \AA}^3$ per iron ion, a little higher than the typical values for a complete LS–HS transition (near 30 \AA^3 per iron atom).^{4(d)}

Unexpectedly, the refined “thermal factor” undergoes an increase between 150 and 100 K as shown in Figure 6. The diffraction patterns taken at 200 K (HS) and 100 K (end of the plateau) are shown in Figure 4. There is a decrease of the intensity of all the high-angle Bragg reflections at 100 K with respect to those at 200 K, which is in agreement with a lower “thermal factor” at 200 K, discarding a bad artifact of the refinement. The higher thermal factor at 100 K is consistent with having the average Fe–N distance coming from the presence of iron ions in two distinct spin states in the same crystallographic position, since no superstructure reflections have been detected. The “thermal factor” is $B = 8\pi^2 \langle u^2 \rangle$ where $\langle u^2 \rangle$ is the quadratic average displacement of each atom with respect to the mean position, in our case due to disorder induced by the presence of HS and LS states.

The disorder can be explained, like in previously reported examples,²⁵ as a result of an antiferromagnetic-like short-range interaction between LS and HS species efficiently transmitted via the cyanide bridges of the polymeric network. The LS–HS transition goes along with a drastic change in the Fe–N distances. The short-range order produced by this interaction gives an intermediate phase in which half of the iron ions are in HS state and another half in LS state. The position of the atoms would also be somewhat disordered near an average

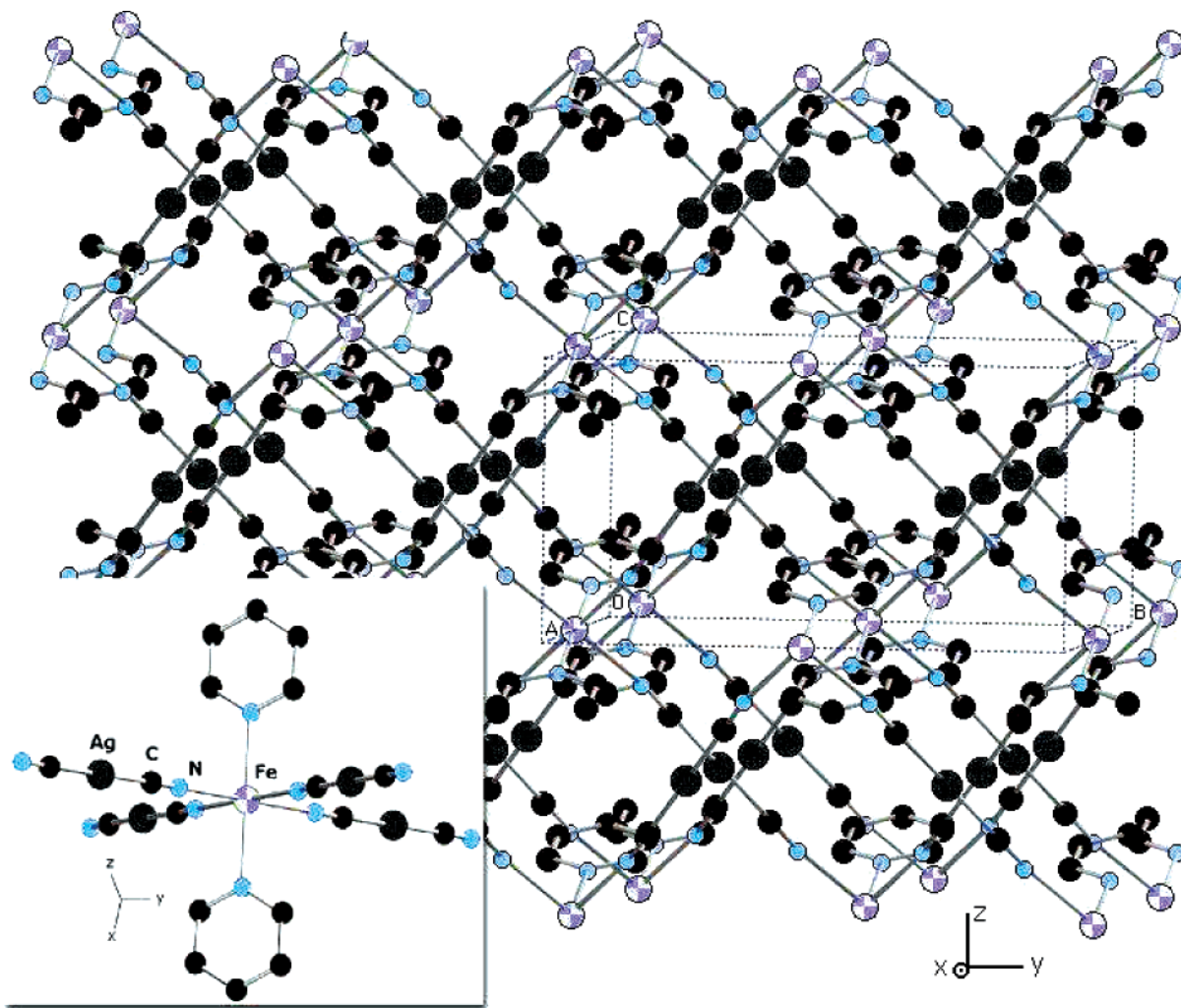


Figure 5. View of the structure of $\text{Fe}(\text{py})_2[\text{Ag}(\text{CN})_2]_2$. Inset: Coordination environment of the Fe atom.

TABLE 2: Crystallographic Data and Reliability Factors²⁰

$T(\text{K})$	200	125	77
space group	$C2/m$	$C2/m$	$C2/m$
$a(\text{\AA})$	8.4799(16)	8.3599(11)	8.2737(15)
$b(\text{\AA})$	13.8959(19)	13.735(2)	13.592(3)
$c(\text{\AA})$	7.3088(14)	7.1842(11)	7.0967(17)
$\beta(^{\circ})$	94.293(12)	94.759(10)	95.118(14)
$V(\text{\AA}^3)$	858.8(3)	822.1(2)	794.9(3)
R_p/R_{wp}	7.72/9.76	7.61/9.62	9.04/11.3
R_{exp}/R_{Bragg}	8.35/6.30	8.71/5.62	8.80/5.61
χ^2	1.36	1.22	1.64
B	9.3(3)	8.5(3)	10.0(4)

position, specially near the iron, what would be interpreted as a large “thermal factor” by the Rietveldt refinement program of a powder pattern. A similar type of disorder has been recently reported in single-crystal samples by Matouzenko et al.¹⁴ and Ortega-Villar et al.¹³ In the latter, the authors detect an anomalous behavior of the thermal parameters of some nitrogen atoms when cooling across the two-step transition. The high thermal parameters are related with a dynamic disorder that becomes static at low temperature. In our compound, the anomalous increase of B between 150 and 100 K ($\Delta B \approx 3$) corresponds to a mean displacement of 0.20 Å, of the order of the change of the Fe–N distance upon the HS–LS transition. The absence of superstructure reflections and the double step observed by various techniques are also explained.

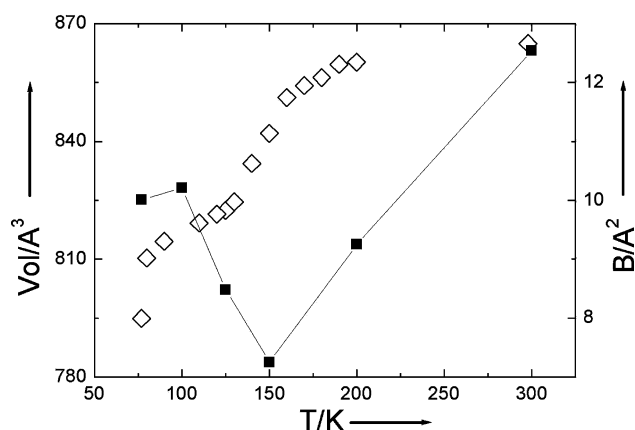


Figure 6. Volume change of the unit cell (\diamond) and thermal parameter B/A^2 (\blacksquare) obtained by X-ray diffraction.

IV. Conclusion

In summary, a new two-dimensional polymeric spin-crossover compound, $\text{Fe}(\text{py})_2[\text{Ag}(\text{CN})_2]_2$, has been synthesized, which is isostructural with a previously reported one in which Cd replaces Fe.¹⁷ Iron occupies only one crystallographic site at every temperature. Calorimetric and magnetic measurements show that this compound undergoes an incomplete two-step spin-crossover transition. The powder X-ray diffraction study at different

temperatures can be explained with a disordered state at the plateau between the two steps, consisting in a random mixing of HS and LS species at a long-range scale. The disorder is manifested through a "thermal factor" that increases while temperature decreases, and by the absence of superstructure peaks in the diffraction pattern. Efforts are in progress to obtain single crystals, which can give a definitive insight into the origin of the two-step transition.

Acknowledgment. We thank the Spanish Ministerio de Educación y Ciencia for J.A.R.V. predoctoral fellowship and financial support through project MAT 2004-03395-C02-02, and the European network of excellence 515767-2 MAGMANet.

References and Notes

- (1) Gütllich, P.; Goodwin, H. A. *Top. Curr. Chem.* **2004**, 233, 1.
- (2) Létard, J. F.; Guionneau, P.; Goux-Capes, L. *Top. Curr. Chem.* **2004**, 234, 221.
- (3) Real, J. A.; Gaspar, A. B.; Muñoz, M. C. *Dalton Trans.* **2005**, 2062.
- (4) (a) Matouzenko, G. S.; Létard, J. F.; Lecocq, S.; Bousseksou, A.; Capes, L.; Salmon, L.; Perrin, M.; Kahn, O.; Collet, A. *Eur. J. Inorg. Chem.* **2001**, 2935. (b) Boïnard, D.; Bousseksou, A.; Dworkin, A.; Savariault, J. M.; Varret, F.; Tuchagues, J. P. *Inorg. Chem.* **1994**, 33, 271. (c) García, Y.; Kahn, O.; Rabardel, L.; Chansou, B.; Salmon, L.; Tuchagues, J. P. *Inorg. Chem.* **1999**, 38, 4663. (d) Niel, V.; Thompson, A. L.; Goeta, A. E.; Enachescu, C.; Hauser, A.; Galet, A.; Muñoz, M. C.; Real, J. A. *Chem. Eur. J.* **2005**, 11, 2047.
- (5) Amooore, J. J. M.; Kepert, C. J.; Cashion, J. D.; Moubarak, B.; Neville, S. M.; Murray, K. S. *Chem. Eur. J.* **2006**, 12, 8220.
- (6) (a) Real, J. A.; Bolvin, H.; Bousseksou, A.; Dworkin, A.; Kahn, O.; Varret, F.; Zarembowitch, J. *J. Am. Chem. Soc.* **1992**, 114, 4650. (b) Real, J. A.; Zarembowitch, J.; Kahn, O.; Solans, X. *Inorg. Chem.* **1987**, 26, 2939. (c) Real, J. A.; Castro, I.; Bousseksou, A.; Verdager, M.; Burriel, R.; Castro, M.; Linares, J.; Varret, F. *Inorg. Chem.* **1997**, 36, 455. (d) Ksenofontov, V.; Gaspar, A. B.; Real, J. A.; Gütllich, P. *J. Phys. Chem. B* **2001**, 105, 12266.
- (7) Real, J. A.; Gaspar, A. B.; Muñoz, M. C.; Gütllich, P.; Ksenofontov, V.; Spiering, H. *Top. Curr. Chem.* **2004**, 233, 167.
- (8) Köppen, H.; Müller, E. N.; Köhler, C. P.; Spiering, H.; Meissner, E.; Gütllich, P. *Chem. Phys. Lett.* **1982**, 91, 348.
- (9) Spiering, H.; Kohlhaas, T.; Romstedt, H.; Hauser, A.; Brun-Yilmaz, C.; Kusz, J.; Gütllich, P. *Coord. Chem. Rev.* **1999**, 192, 629.
- (10) Chernyshov, D.; Hostettler, M.; Törnroos, K. W.; Bürgi, H. B. *Angew. Chem. Int. Ed.* **2003**, 42, 3825.
- (11) Kusz, J.; Schollmeyer, D.; Spiering, H.; Gütllich, P. *J. Appl. Cryst.* **2005**, 38, 528.
- (12) Grunert, M.; Schweifer, J.; Weinberger, P.; Linert, W. *Inorg. Chem.* **2004**, 43, 155.
- (13) Ortega-Villar, N.; Thompson, A. L.; Muñoz, M. C.; Ugalde-Saldivar, V. M.; Goeta, A. E.; Moreno-Esparza, R.; Real, J. A. *Chem. Eur. J.* **2005**, 11, 5721, and references therein.
- (14) Matouzenko, G. S.; Luneau, D.; Molnár, G.; Ould-Moussa, N.; Zein, S.; Borshch, S. A.; Bousseksou, A.; Averseng, F. *Eur. J. Inorg. Chem.* **2006**, 2671.
- (15) Kitazawa, T.; Gomi, Y.; Takahashi, M.; Takeda, M.; Enomoto, M.; Miyazaki, A.; Enoki, T. *J. Mater. Chem.* **1996**, 6, 119.
- (16) Galet, A.; Niel, V.; Muñoz, M. C.; Real, J. A. *J. Am. Chem. Soc.* **2003**, 125, 14224.
- (17) Soma, T.; Iwamoto, T. *J. Inclusion Phenom. Mol. Rec.* **1996**, 26, 161.
- (18) Pavese, F.; Malyshev, V. M. *Adv. Cryog. Eng.* **1994**, 119.
- (19) Palacios, E.; Melero, J. J.; Burriel, R.; Ferloni, P. *Phys. Rev. B* **1994**, 54, 9099.
- (20) Rodríguez-Carvajal, J. L.; Anne, M.; Pannetier, J. FULLPROF. ILL Report 87 R014T, (updated as FullProf.2k version 2.20, 2002), 1987.
- (21) Roubeau, O.; Stassen, A. F.; Gramage, I. F.; Codjovi, E.; Linares, J.; Varret, F.; Haasnoot, J. G.; Reedijk, J. *Polyhedron* **2001**, 20, 1709.
- (22) Hinek, R.; Gütllich, P.; Hauser, A. *Inorg. Chem.* **1994**, 33, 567.
- (23) Sorai, M. *Top. Curr. Chem.* **2004**, 235, 153.
- (24) Bak, B.; Hansen, L.; Rastrup Andersen, J. *J. Chem. Phys.* **1954**, 22, 2013.
- (25) Romstedt, H.; Hauser, A.; Spiering, H.; Gütllich, P. *J. Phys. Chem. Solids* **1998**, 59, 1353.